ExtravDose Modeling Theory

for VARSKIN+ (V+) Version 2.0, software release: April 1, 2025

Roland Benke, PhD, CHP

Director – Technologies Division
roland.benke@rcdsoftware.com

David Hamby, PhD

Founder & Operations Manager
david.hamby@rcdsoftware.com

Disclaimer

This presentation is an independent product of RCD and does not communicate the views or positions of the U.S. Nuclear Regulatory Commission (NRC).

Training Progression for ExtravDose

RCD

Training on theory covers multiphysics mathematical models for fluid flow, activity concentrations, and dosimetry

← You are here.

Beginner training emphasizes Basic calculation

Intermediate training includes Advanced calculation features

ExtravDose discussions

Outline for Training on Theory

Part I

- Event Overview
- Variables to Consider
- Clinical Insights for Dose Modeling in Recent Literature

Part II

- Multiphysics Modeling Overview
- Extravasated Fluid Flow in Tissue
- Activity Concentration in Tissue

Part III

- Photon Dosimetry
- Electron Dosimetry
- Alpha Particle Dosimetry

Part I

– Extravasation dosimetry module

Extravasation occurs when radiopharmaceutical intended for the bloodstream leaks into surrounding tissue.

Temporary condition that elevates absorbed radiation dose to healthy tissue without a medical benefit

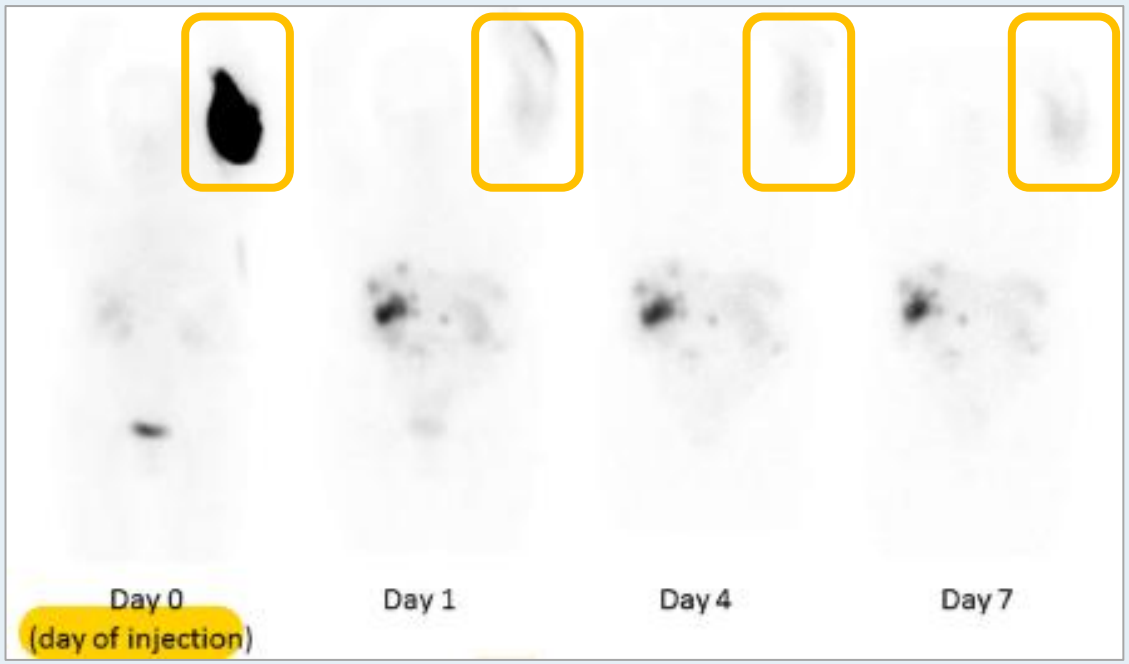

Arveschoug *et al. EJNMMI Research* (2020) 10:68
https://doi.org/10.1186/s13550-020-00658-6

OBJECTIVE

Develop models for a computational tool (software) to calculate 3D dose distributions in tissue with interfaces and flexibility appropriate for radionuclide extravasations

V+ software is available from U.S. NRC https://ramp.nrc-gateway.gov/

What matters for modeling?

- Physical and chemical characteristics of the radiopharmaceutical
- Administration flow rate and duration (gravity method, infusion pump, injection)
- Biological composition and structure at the site of extravasation (tissue matrix)
- Physical changes to the site (elevation of site, warm compress)
- Biophysical movement and dissipation of extravasated fluid (flow & removal)
  - Volume of tissue affected by extravasated fluid
  - Extravasated fluid concentrations in tissue over time
- Radioactivity extravasated (initial source term)
- Radioactive decay, emission type and energy

Multiphysics aspects addressed in 3 models

Flow Model	Movement of radioactive extravasated fluid in tissue
Activity Concentration Model	Activity concentration in tissue over time in three dimensions
Dosimetry Model	Local tissue dose over time in three dimensions

Characterization of PET Extravasation (1 of 3)

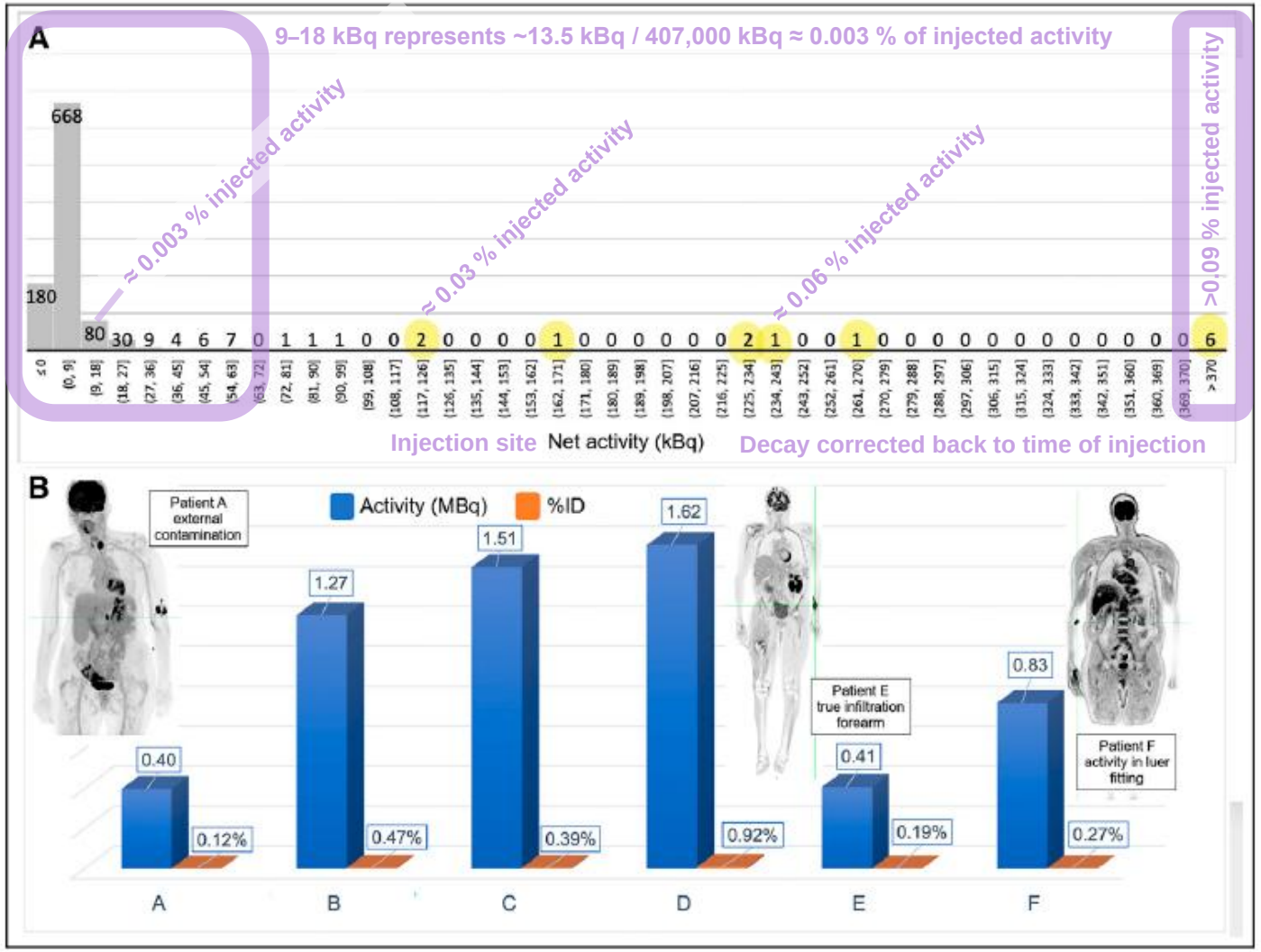

FIGURE 2. (A) Histogram distribution of net activity (MBq) at injection site. (B) Detail of 6 infiltrations above 0.4 MBq (10 μCi) with percentage injected activity. Patient E's injection geometry was used in Monte Carlo simulation.

Characterized 1,000 patient injections at more than 10 imaging locations

- Primarily ^{18}F, some ^{68}Ga administrations
- Average injected activity was 407 MBq

Whole-body planar imaging

- Performed 3-4 h after injection
- Determined activity retained at injection site
- Estimated volume of tissue infiltrated by extravasated fluid

No patient retained more than 1% at injection site

Sutherland et al. (2023) Multicenter Evaluation of Frequency and Impact of Activity Infiltration in PET Imaging, Including Microscale Modeling of Skin-Absorbed Dose. *J Nucl Med* 64: 1095-1101. doi:10.2967/jnumed.123.265891.

Additional commentary provided by Knowland et al. (2023) Critique and discussion of "Multicenter evaluation of frequency and impact of activity infiltration in PET imaging, including microscale modeling of skin-absorbed dose." *Frontiers in Nuclear Medicine* doi:10.3389/fnume.2023.1240162.

Characterization of PET Extravasation (2 of 3)

"The dermis is a largely dense connective tissue, consisting primarily of collagen and elastin surrounded by glycosaminoglycans (highly polar water-binding molecules) that enable collagen fibers to retain water; this water is not freely exchangeable. For purposes of our dose calculations, hypodermis-to-dermis radioactivity concentration ratios of 10:1, 5:1, and 2:1 were simulated, but the results from the 10:1 simulations are likely closest to reality."

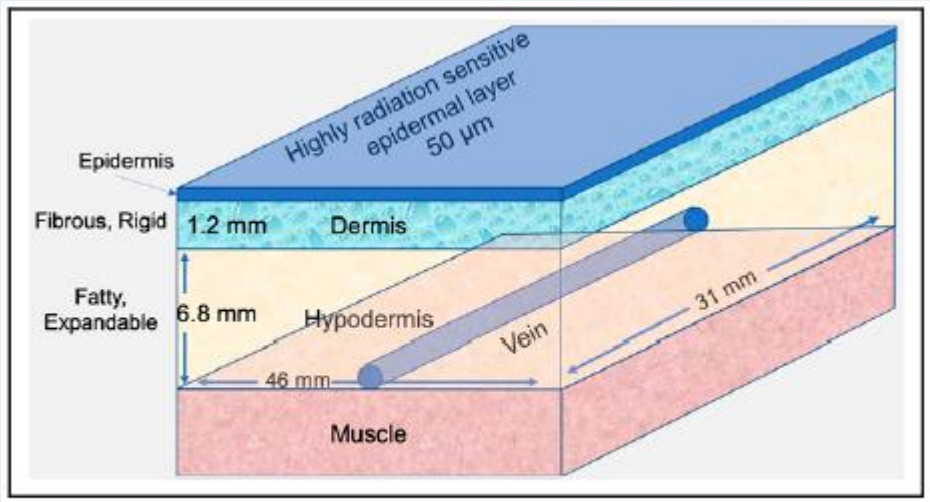

FIGURE 1. Schematic of skin anatomy with primary dimensions used in Monte Carlo absorbed dose calculations.

Sutherland et al. (2023) Multicenter Evaluation of Frequency and Impact of Activity Infiltration in PET Imaging, Including Microscale Modeling of Skin-Absorbed Dose. *J Nucl Med* 64: 1095-1101. doi:10.2967/jnumed.123.265891.

Characterization of PET Extravasation (3 of 3)

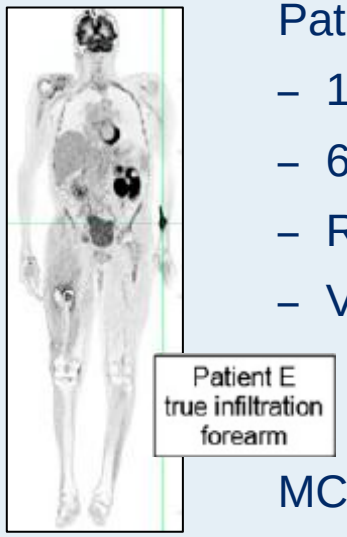

Patient-specific micro-dosimetry analysis

- 1.2 mm dermis
- 6.8 mm subcutaneous layer (from CT images)
- Radioactivity remaining at injection site, 0.19% injected activity
- Volume of tissue infiltrated, 3.6 cm × 2.1 cm

MCNP 6.2 modeling of absorbed dose to different tissue layers

- Assumed static activity distribution in hypodermis & dermis
- Assigned 10:1, 5:1, 2:1 hypodermis:dermis ratios for activity partitioning
- Authors preferred 10:1 based on animal experiments
- Effective half-lives: 25 min for ^{68}Ga & 30 min for ^{18}F from literature

Highlighted need for quantitative measurements of activity partitioning between subcutaneous tissue & dermis

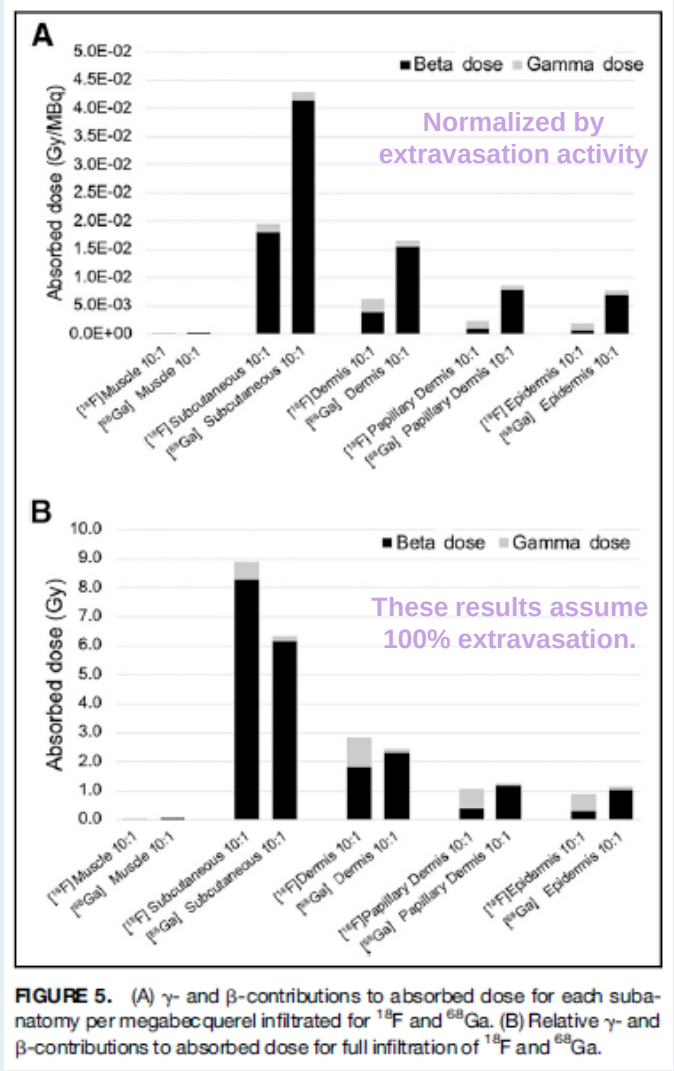

FIGURE 5. (A) γ- and β-contributions to absorbed dose for each subanatomy per megabecquerel infiltrated for ^{18}F and ^{68}Ga. (B) Relative γ- and β-contributions to absorbed dose for full infiltration of ^{18}F and ^{68}Ga.

Sutherland et al. (2023) Multicenter Evaluation of Frequency and Impact of Activity Infiltration in PET Imaging, Including Microscale Modeling of Skin-Absorbed Dose. *J Nucl Med* 64: 1095-1101. doi:10.2967/jnumed.123.265891.

Biological clearance of ^{18}F-FDG from extravasation site

Ören et al. (2017) IDACSTAR: A MCNP application to perform realistic dose estimations from internal or external contamination of radiopharmaceuticals. *Radiation Protection Dosimetry.* 174(3): 406-411. doi:10.1093/rpd/ncw221.

For the extravasation, the effective dose was estimated to be 1.6 mSv assuming that all the activity being absorbed within the site of the extravasation. The activity in the extravasation area was estimated from the clinical images to be 90 MBq of ^{18}F-FDG 87 minutes after the 370 MBq administration. Assuming a bi-exponential retention of the activity from the extravasation site to the blood, a biological half-time of 70 minutes was estimated. The effective dose for the more realistic case, where a fraction of 0.39 of the total number of disintegrations was in the extravasation volume, was estimated to be 4.5 mSv.

- Activity estimated from clinical images
- Bi-exponential retention at extravasation site
- ^{18}F-FDG biological half-time ~ 70 min

Andersson et al. (2022) IDACstar2.0: A MCNP application to perform realistic dose estimations from internal or external contamination with radiopharmaceuticals. *Radiation Physics and Chemistry.* https://doi.org/10.1016/j.radphyschem.2021.109957.

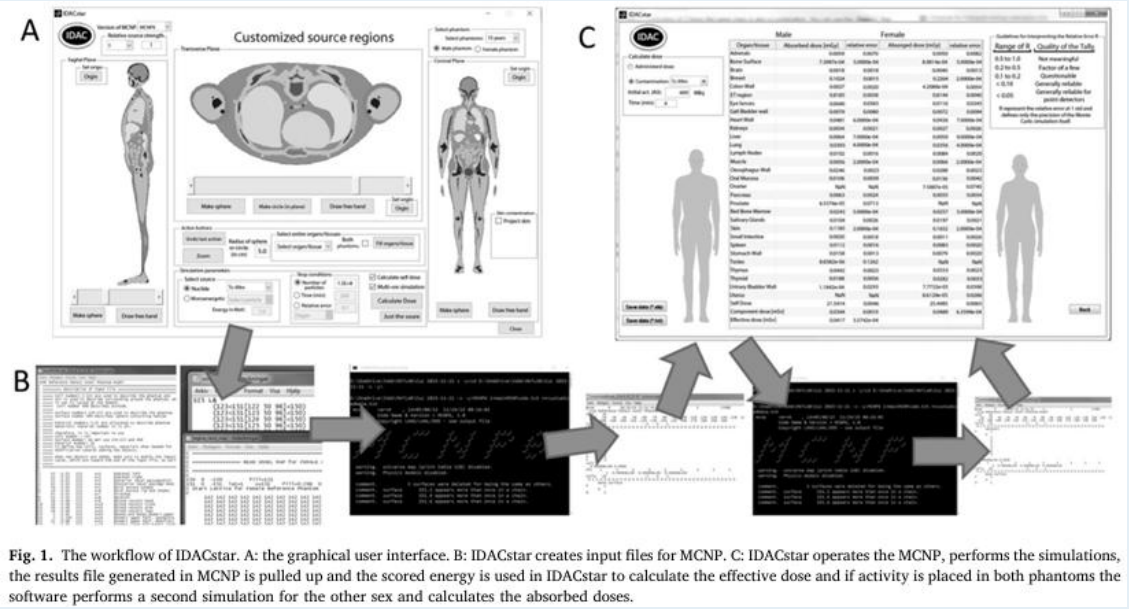

Fig. 1. The workflow of IDACstar. A: the graphical user interface. B: IDACstar creates input files for MCNP. C: IDACstar operates the MCNP, performs the simulations, the results file generated in MCNP is pulled up and the scored energy is used in IDACstar to calculate the effective dose and if activity is placed in both phantoms the software performs a second simulation for the other sex and calculates the absorbed doses.

Graphical user interface creates input files for MCNP.

Papers address effective (whole-body) doses, not yet optimized for extravasation dose to local tissue.

Extravasation modeling from PET/CT imaging (1 of 3)

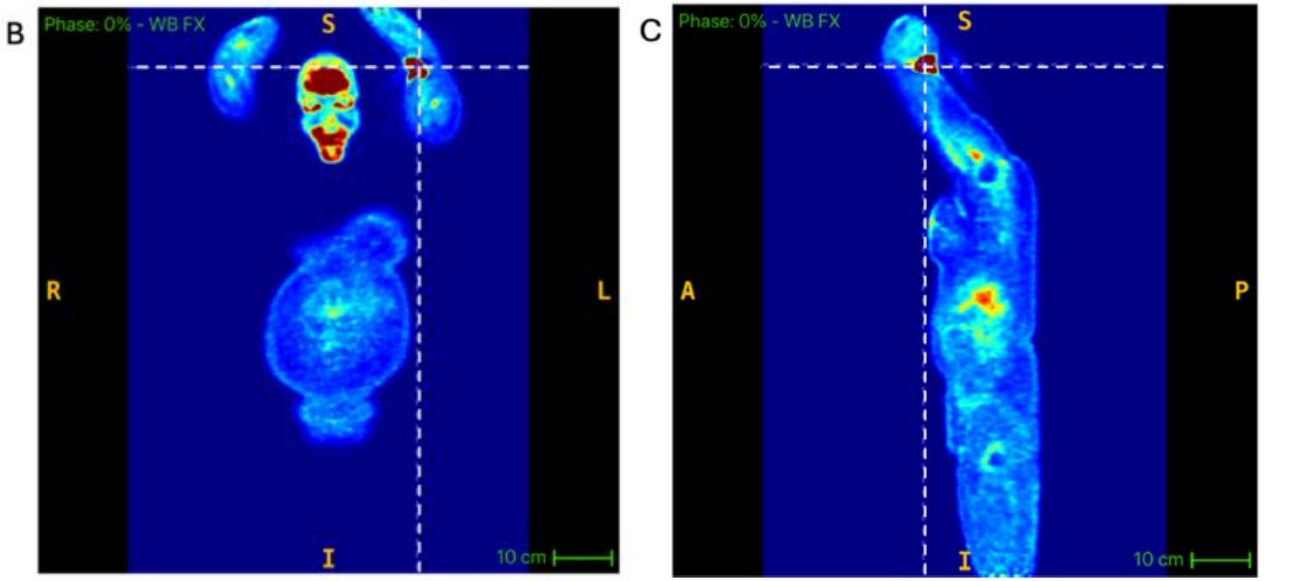

Fig. 1. ITK-SNAP [Paul et al., 2006] CT views of the injected patient. PET-CT images (A: axial, B: coronal, C: sagittal) showing the distribution of 18F-FDG radiopharmaceutical, with a notable accumulation in the extravasation region (e.g. dashed line points to the Region Of Interest, ROI).

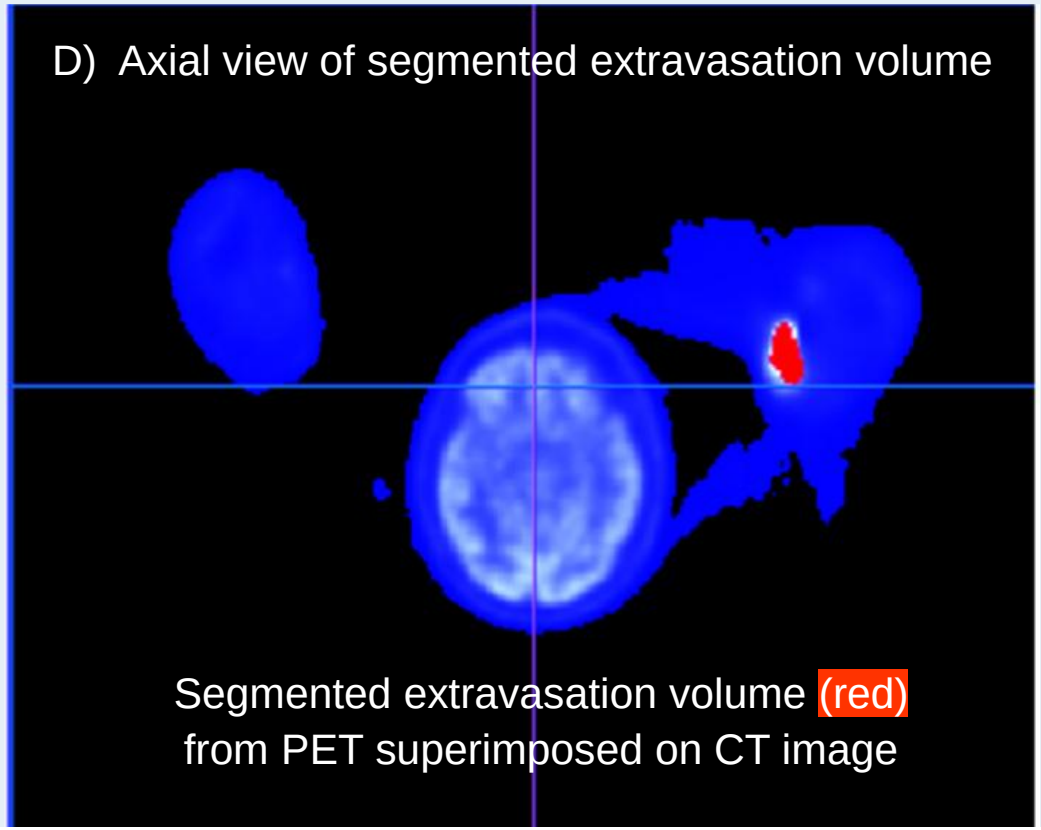

Fig. 2. Build-up phases for the generation of the FE model with Synopsys® Simpleware™ Medical. Panel A) Axial, B) Coronal, C) Sagittal CT views with evidence of the implemented segmentation of the tissues; ochre, skin; green, adipose tissue; red, muscle; pearl, bone. D) Axial view of the segmented extravasation volume superimposed on the CT image from the PET analyses, colors chosen to make evident the ROI. The legs were excluded from the FE model used for transport simulations obtaining a more manageable computational model, while preserving details of the of the ROI and critical organs in the upper body portion. (For interpretation of the references to color in this figure legend, the reader is referred to the Web version of this article.)

Isolan et al. (2025) Extravasation Modeling from a PET/CT Imaging for a Possible Digital Twin Approach. *Radiation Physics and Chemistry.* https://doi.org/10.1016/j.radphyschem.2025.113080.

Extravasation modeling from PET/CT imaging (2 of 3)

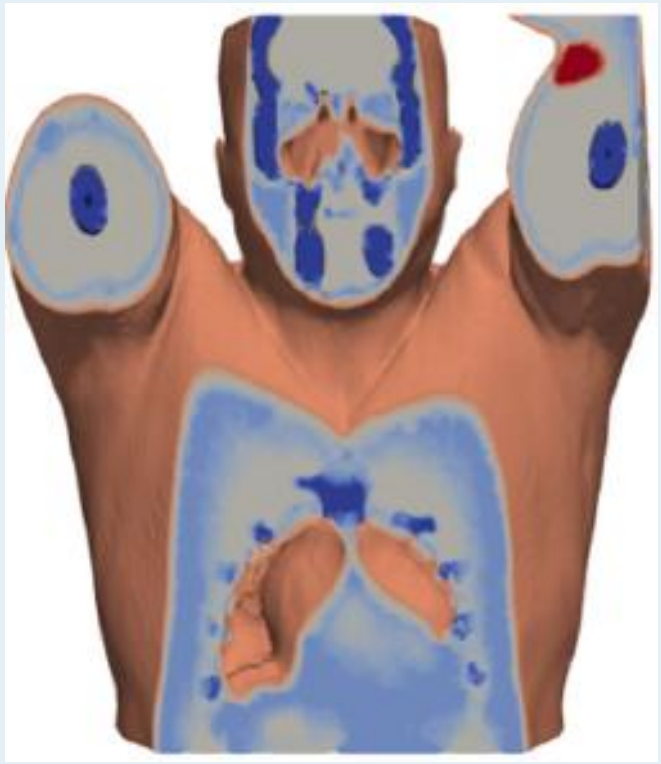

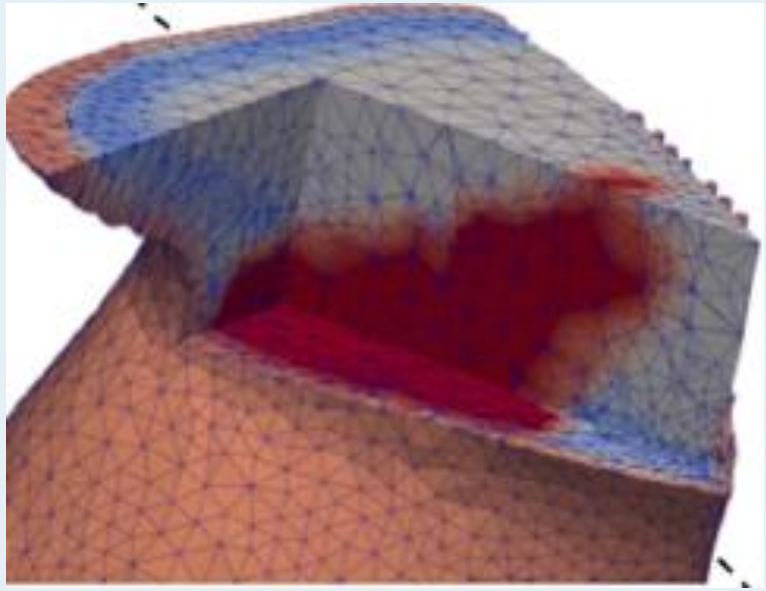

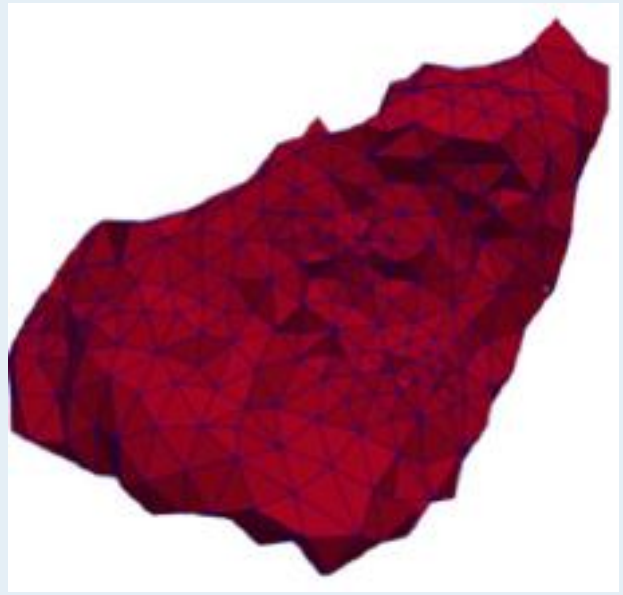

Fig. 3. The MCNP6.2© model. A) UM of the patient, magnification on the meshed extravasation region embedded in the left arm, extravasation region volume (corresponding to the source of particles thanks to the VOLUMER keyword). B), C), D), different views of the model with evidence of some cuts in the geometry to put in evidence the complex internal structures and the extravasation region/source; de-facing mask applied. Red, extravasation; Pink, skin; Dark blue, bone; Light blue, adipose tissue; ice color, muscle. Each color/tissue identifies a transport domain. See Table 1. (For interpretation of the references to color in this figure legend, the reader is referred to the Web version of this article.)

- Digital twin with four million spatial elements & related nodes for MCNP 6.2 dose modeling
- Incorporated ^{18}F-FDG (fluorodeoxyglucose) effective half-life & mixing with blood
- Model imagery appears to show infiltration in dermis, hypodermis, and portion of adjacent muscle

Isolan et al. (2025) Extravasation Modeling from a PET/CT Imaging for a Possible Digital Twin Approach. *Radiation Physics and Chemistry.* https://doi.org/10.1016/j.radphyschem.2025.113080.

Extravasation modeling from PET/CT imaging (3 of 3)

Applied effective half-life from literature to total radioactivity in infiltrated volume over time

Effective half-life ~ 84 min from slope (below)

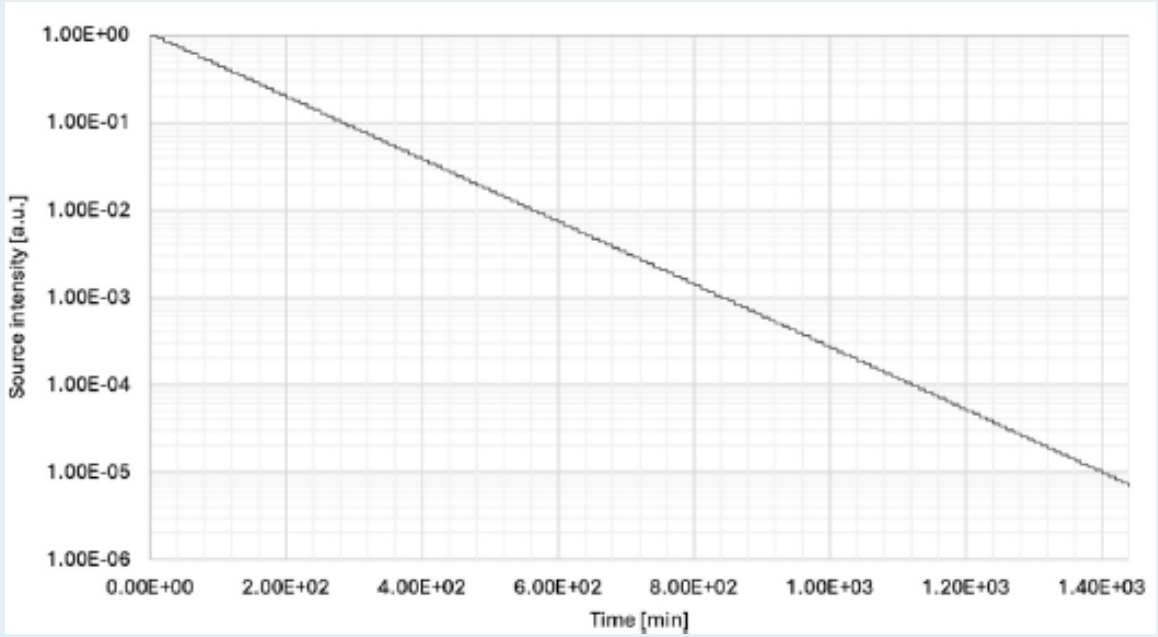

Patient was injected with 227 MBq ^{18}F-FDG

228 mGy dose to extravasation volume

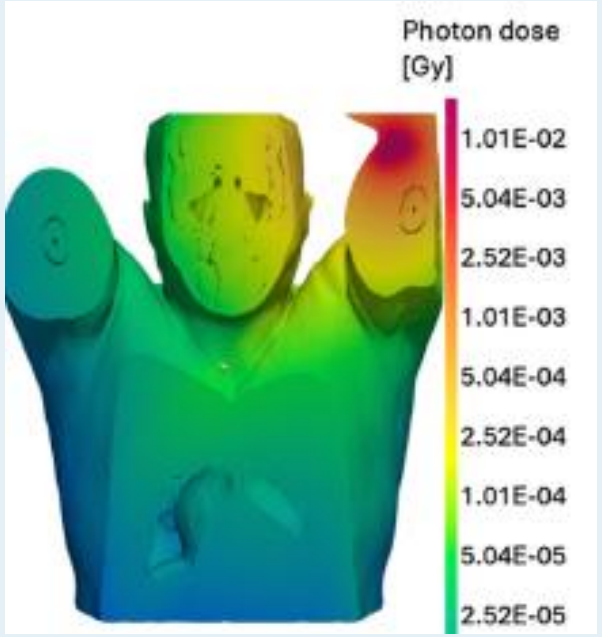

(from Figs. 4 & 5) Isolan et al. (2025) Extravasation Modeling from a PET/CT Imaging for a Possible Digital Twin Approach. *Radiation Physics and Chemistry.* https://doi.org/10.1016/j.radphyschem.2025.113080.

^{99m}Tc-HDP effective half-life at extravasation site

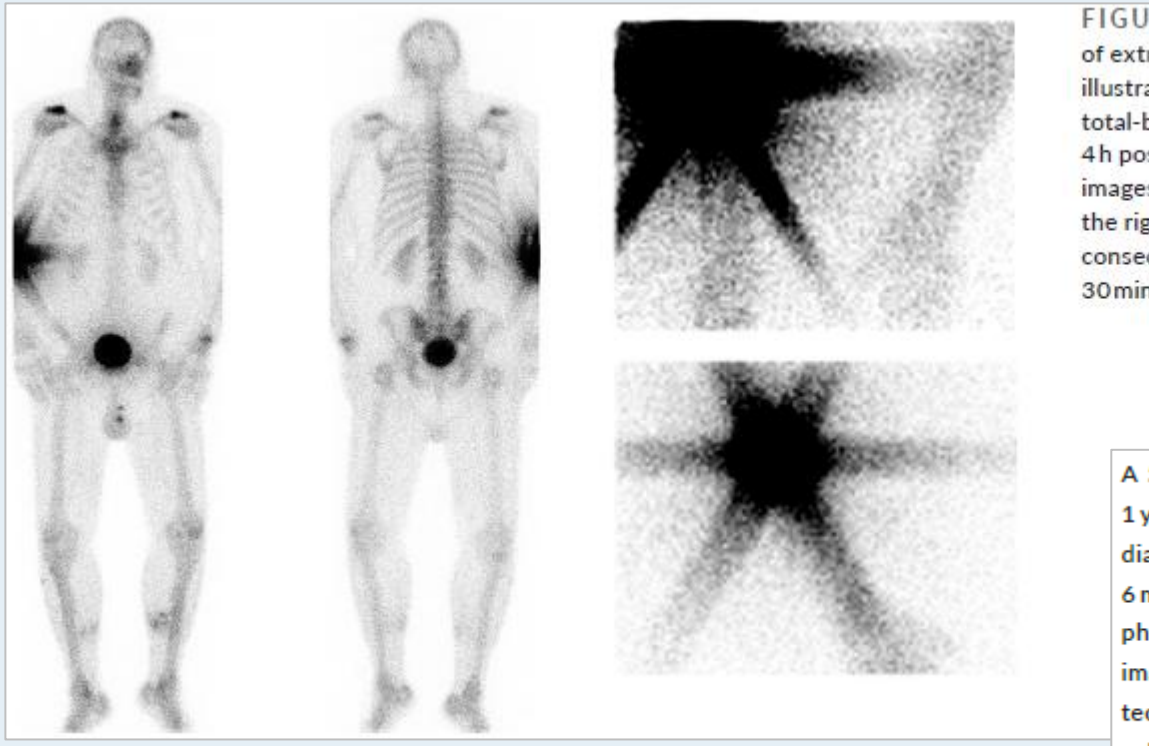

FIGURE 1 High activity at the site of extravasation in the right elbow is illustrated on anterior and posterior (AP) total-body planar scintigraphy images 4 h post-extravasation (left); and anterior images of the (AP) planar imaging of the right elbow injection site used for consequent dosimetry calculation, at 30 min (top right) and 4 h (bottom right).

- ^{99m}Tc-HDP effective half-life ~ 90 min
- Relatively simple modeling assumptions
- Local tissue doses not summarized here

A 50-year-old male patient presented with pain and dysfunction 1 year after a left-sided distal radius fracture. In order to better diagnose and treat the patient, 871 MBq [99mTc]Tc-HDP (volume 6 mL, body weight 130 kg) was administered to perform three-phase bone scintigraphy.[1] After intravenous injection, dynamic imaging showed no visual activity at the wrist. This prompted the technician to suspect an extravasation. This extravasation was subsequently investigated further using planar imaging of the injection site (Figure 1).

Doornhof et al. (2024) Treatment of [99mTc]Tc-hydroxy-diphosphonate ([99mTc]Tc-HDP) extravasation using hyaluronidase. *Pharmacol Res Perspect.* 2024;12:e1232. https://doi.org/10.1002/prp2.1232.

Extravasation in ^{177}Lu-DOTATATE therapy

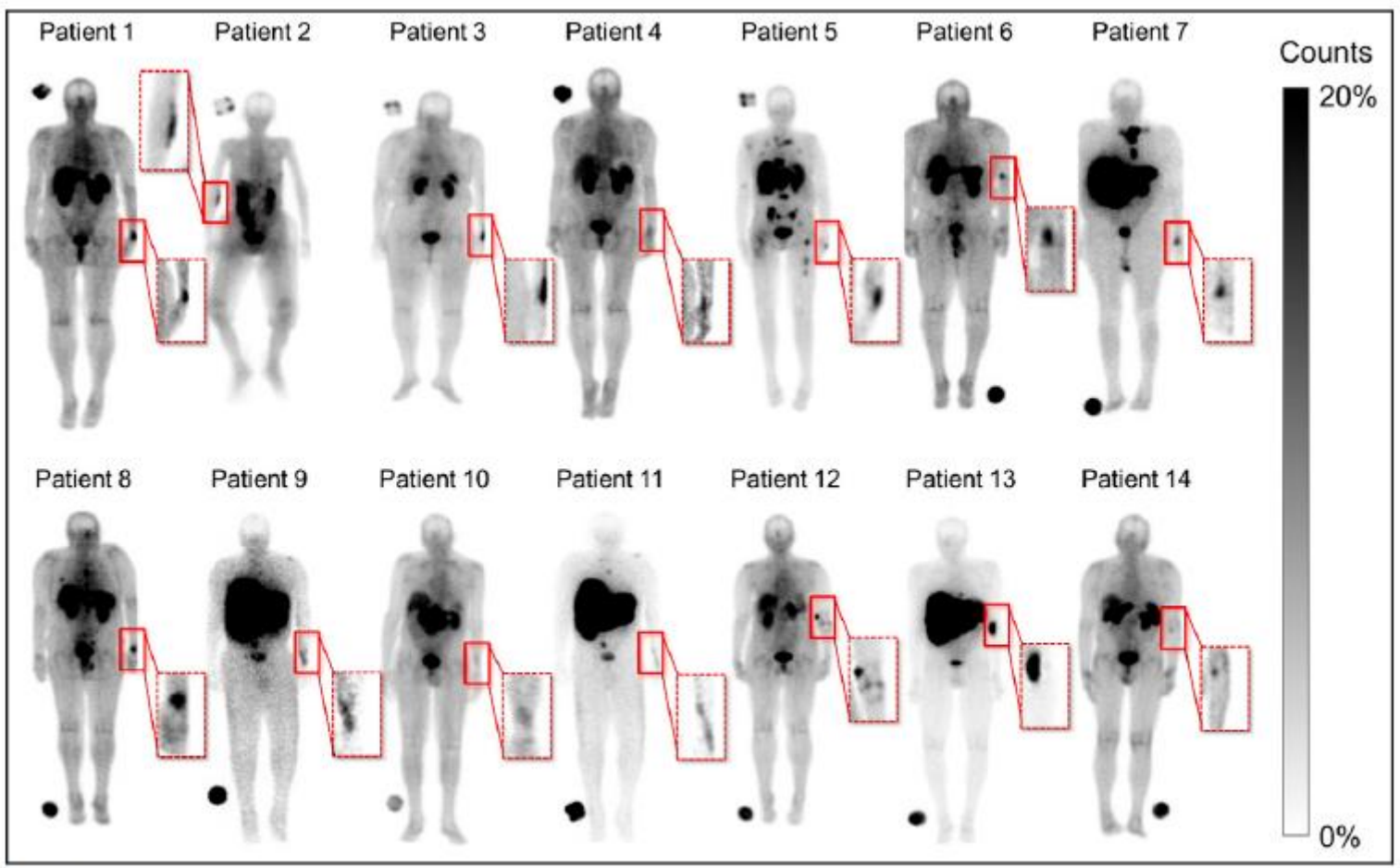

FIGURE 1. Planar gamma camera images (conjugate view geometric mean) of 14 patients with identified extravasations (highlighted in red dashed box) acquired using Philips XCT (patients 1–4) and Siemens Symbia 1 and 2 SPECT/CT systems (patients 5–14). All patients, except patient 2, had infusion in left arm. Gray scale was narrowed to 20% to enhance visualization of extravasations.

- Whole-body planar imaging performed 3-4 h after injection
- Extravasation occurs in hypodermis
- Homogeneous activity distribution assumed
- No patients retained more than 1% at injection site at time of scan
- No adverse skin reactions found within days to weeks
- Rapid dispersal from concurrent saline infusion & small molecule pharmacokinetics

Kayal et al. (2025) Extravasation Frequency of [^{177}Lu]Lu-DOTATATE: Insights and Implications Derived from 1,314 Cycles of Treated Patients—A Single-Site Analysis. *J Nucl Med* doi:10.2967/jnumed.124.269411. June 26, 2025.

Part II

Flexible tissue layering

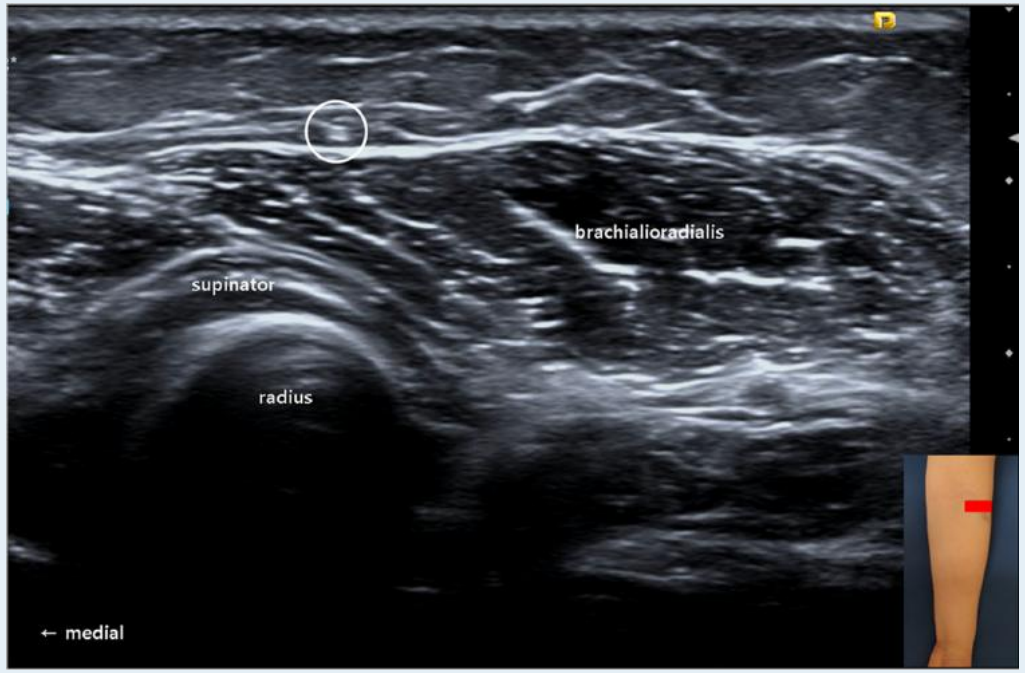

Kwak and Chang (2020) Compression of the lateral antebrachial cutaneous nerve due to leakage of iron after an intravenous iron infusion. *Diagnostics* 2020, 10, 516. Figure 1(C).

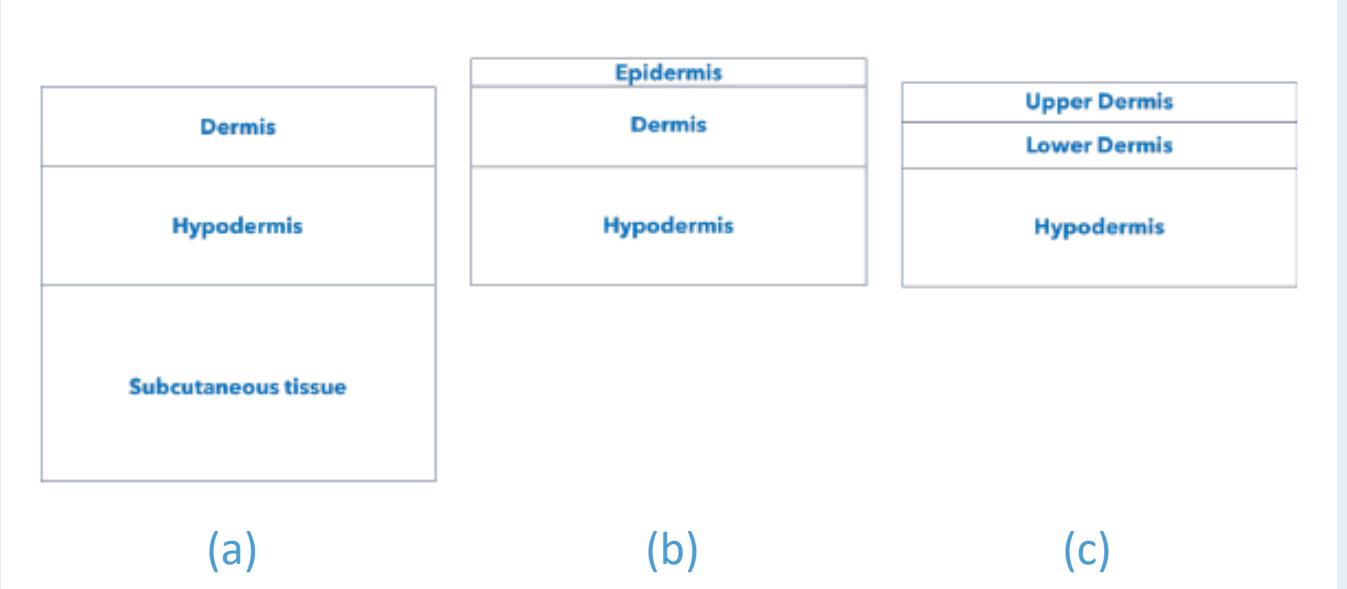

accommodates

- (a) Deep infiltration without appreciable extravasation in epidermis
- (b) Dermal extravasation with explicit infiltration into the epidermis
- (c) Confined extravasation within multiple dermal layers

Flow primarily driven by pressure

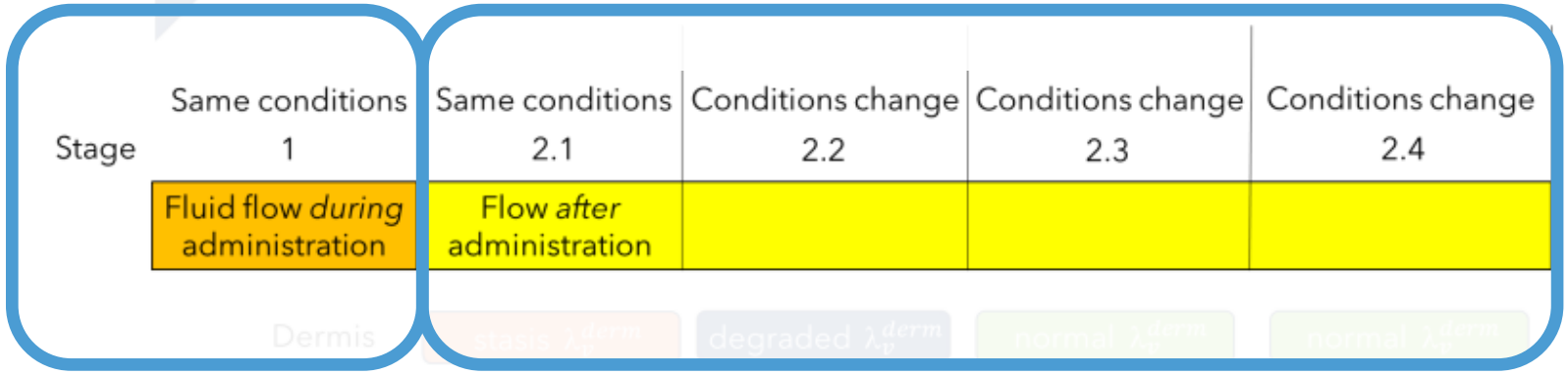

STAGE 1	STAGE 2
External driving force to flow	No external driving force
Theis equation for confined flow	Darcy flow with hydrostatic pressure from fluid in tissue
2D lateral calculation initially + vertical fluid distribution	3D calculation

Discuss each model

Flow Model

Activity Concentration Model

Dosimetry Model

Starting with …

Flow Model Overview

Homogeneous tissue matrix

Interstitial components include fine vascular bathed in extracellular fluid.

before extravasation

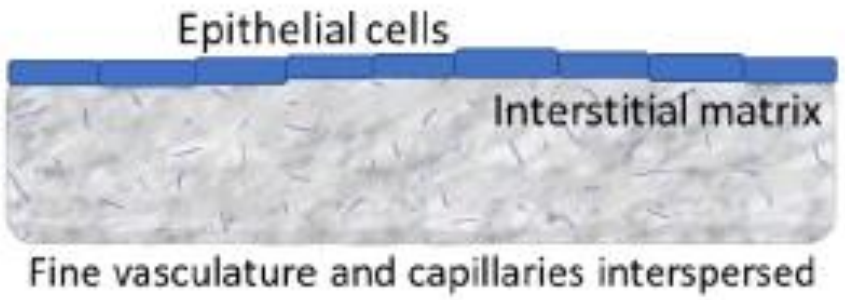

after extravasation

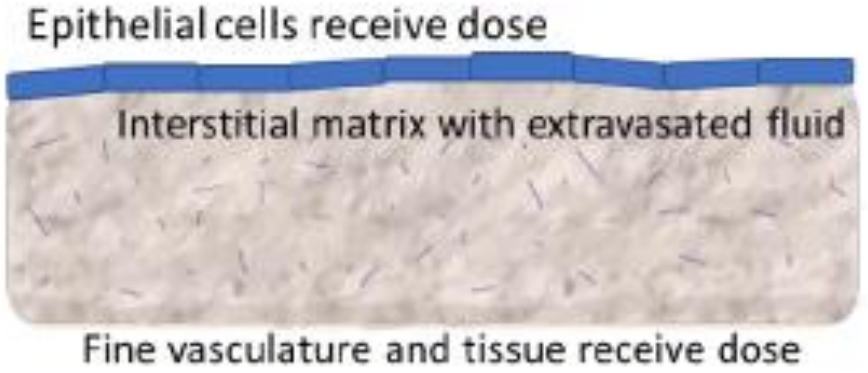

In initial model, fluid movement is tracked in a stationary grid *without* tissue shape changes.

Flow in Stage 1

External driving force to flow

Theis equation for confined flow

2D lateral calculation initially + vertical fluid distribution

Confined flow during administration in Stage 1

The “confined flow” assumption means extravasation flow occurs in the matrix between impermeable layers above (e.g., epidermis) and below (e.g., fibrous connective tissue).

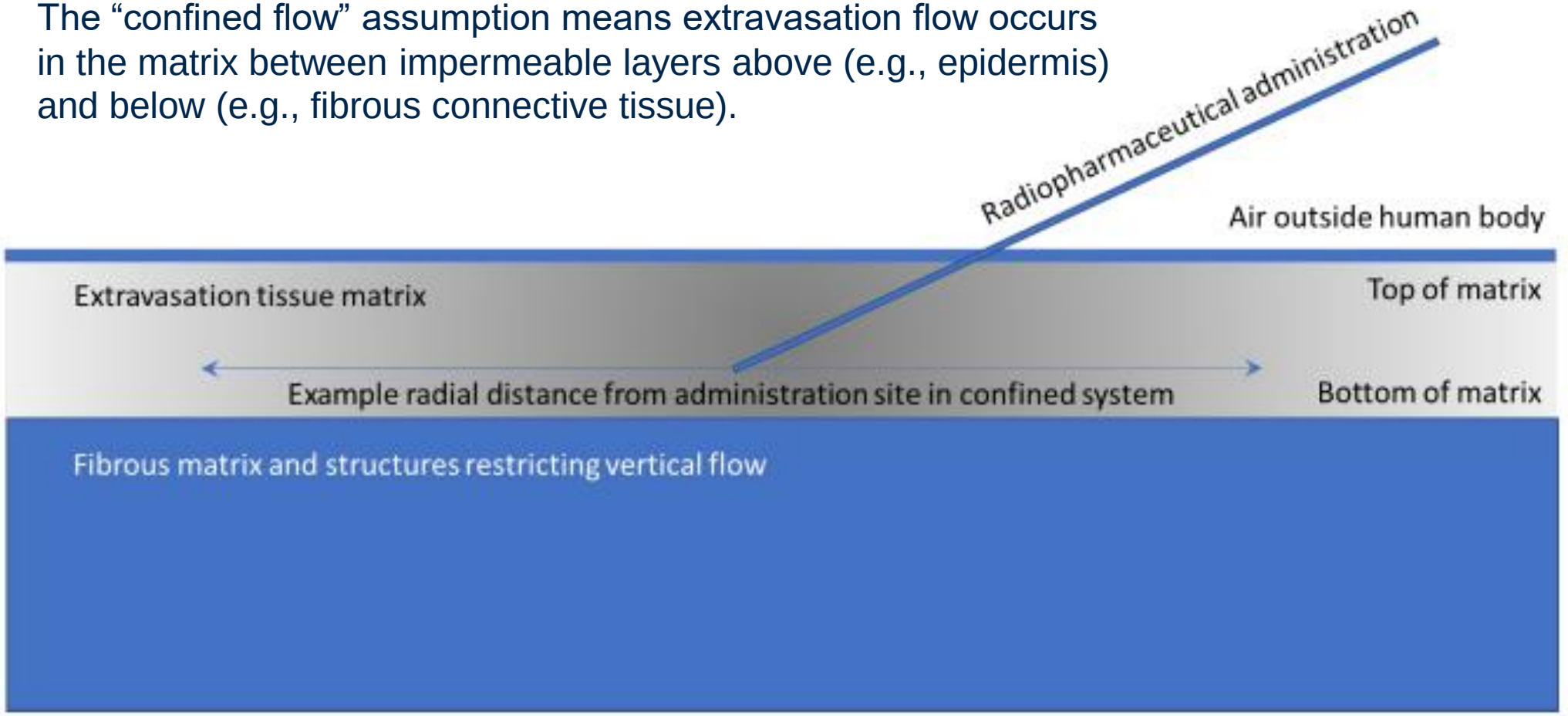

Theis Equation utilized for Stage-1 flow modeling

Hydrostatic pressure head [cm] as function of space and time

$$p(r,t) = \frac{Q}{4\pi T} E_1\left(\frac{S}{4\,T}\frac{r^2}{t}\right)$$

Exponential integral definitions

$$E_n(z) = z^{n-1}\int_z^\infty \frac{e^{-x}}{x^n}dx$$

$$E_1(z) = \int_z^\infty \frac{e^{-x}}{x}dx$$

Q	Extravasation volumetric flow rate [ml h^{-1}]
T	Effective tissue transmissivity for extravasation lateral flow [cm^2 h^{-1}]
S	Storage coefficient for extravasated fluid in tissue [unitless]
r	Radial distance from administration site [cm] and
t	Elapsed time during radiopharmaceutical administration [h]

Storage coefficient is a relatively insensitive parameter for extravasation; therefore $S = 0.02$ (unitless default value).

Darcy Flow & Transmissivity

Darcy flow velocity [cm s^{-1}] depends on pressure differentials and properties of the flow matrix

$$v = -\left(\frac{T}{h}\right)\left(\frac{\Delta p}{\Delta r}\right)$$

h	Effective thickness of tissue for extravasation flow [cm]
Δp	Hydraulic pressure gradient [cm] and
Δr	Distance over which the pressure gradient applies [cm]

$$T = K\ h$$

"Effective" accounts for spatial heterogeneity within the tissue matrix

T	Effective tissue transmissivity for extravasation lateral flow [$cm^2\ h^{-1}$]
K	Effective hydraulic conductivity for a homogeneous tissue matrix [$cm\ h^{-1}$]

Effective Transmissivity for Tissue Layers

$$T = \frac{\sum_{i=1}^{m} h_i T_i}{h}$$

Calculated as a weighted sum of transmissivities for individual layers i

T	Effective transmissivity for lateral flow in the tissue matrix [$cm^2\ h^{-1}$]
h_i	Thickness of i^{th} layer in the tissue matrix receiving extravasated fluid [cm]
T_i	Transmissivity for lateral flow in the i^{th} layer of the tissue matrix [$cm^2\ h^{-1}$]
i	Index representing one of multiple layers [unitless] and
m	Total number of layers in the tissue matrix [unitless]

Infiltrating Fluid Influences Local Transmissivity

To implement lateral flow, transmissivity is adjusted for combined effects of

- Hydraulic conductivity increases in fluid-filled tissue and
- Potentially greater flow heights

$$T = T_0 \cdot x^{\left(\frac{V_k + V_l}{2\ s^3}\right)\left(1\ \frac{\mathrm{cm}^3}{\mathrm{ml}}\right)}$$

Users can specify T_0 and s in advanced calculations.

T_0	Nominal transmissivity of the tissue layer without extravasation [$cm^2\ h^{-1}$]
x	Base of the power relationship [unitless default value of 2 is assumed]
V_k	Extravasated fluid volume in voxel k [ml]
V_l	Extravasated fluid volume in voxel l [ml]
s	Voxel side length [cm]

Lateral Extravasated Fluid Flow during Administration

For a constant volumetric flow rate of the radiopharmaceutical during administration (Stage 1)

- Quasi-steady-state conditions for lateral extravasation flow would be reached within ~5 min
- Simplification is made to remove the time dependence from the Theis equation

Radial pressure gradient from the Theis equation yields a quasi-steady-state velocity profile

$$v = \frac{T}{h}\left[\frac{p(r_0) - p(r_1)}{r_1 - r_0}\right]$$

Radial flow velocity solved at numerous radial positions

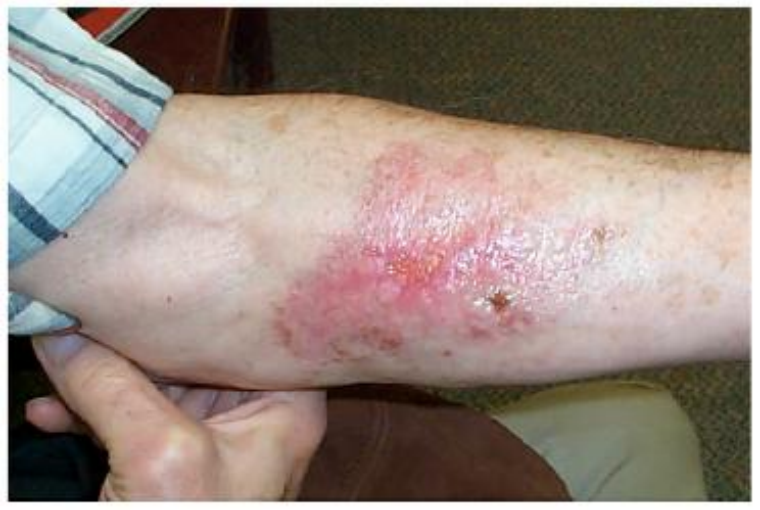

Bonta et al. (2011) Extravasation of a therapeutic dose of ^{131}I-metaiodobenzylguanidine: Prevention, Dosimetry, and Mitigation. *J Nucl Med* 52: 1418-1422.

Extravasated Fluid at Radial Locations Apportioned to Layers Based on Transmissivity

Extravasated fluid volume per unit tissue volume at various radial positions in each layer, $\delta_{r_j,i}$ [ml cm^{-3}]

Calculated by dividing the infiltrating extravasated fluid volume, V_{r_j}, by the original tissue volume of that layer at radial position r_j

Volume of extravasated fluid [ml] in radial ring j is apportioned to layer i

$$\delta_{r_j,i} = \left(\frac{V_{r_j}}{h_i A_{r_j}}\right)\left(\frac{T_i}{\sum_{i=1}^{m} T_i}\right)$$

index $j \in \{0, 1, \ldots, n\}$ for radial rings

index $i \in \{1, \ldots, m\}$ for tissue layers

Tissue volume [cm^3] for layer i within radial ring j

A_{r_j} Cross-sectional area for the j^{th} radial ring [cm^2]

Flow in Stage 2

No external driving force

Darcy flow with hydrostatic pressure from fluid in tissue

3D calculation

Stage 2 Addresses Flow after Administration Ceases

Parameters of state for the computational cell

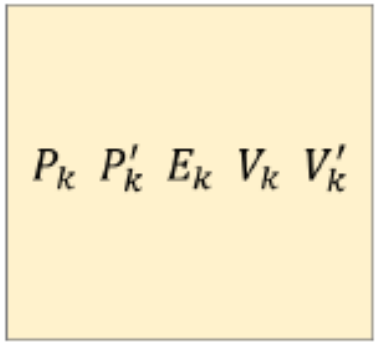

Generic cell index = k

Symbol	Units	Parameter Description
P_k	cm	Hydrostatic pressure head at start of time step
P'_k	cm	Hydrostatic pressure head at end of time step
V_k	ml	Volume of extravasated fluid at start of time step
V'_k	ml	Volume of extravasated fluid at end of time step
E_k	cm	Elevation head relative to administration site

Residual hydrostatic pressure from extravasated fluid temporarily trapped in tissue

$$P_k = 5.70\left[1 - e^{-2.92\left(\frac{V_k}{s^3}\right)}\right]$$

V_k is the extravasated fluid volume in the computational cell at position k [ml]

s^3 represents the volume of one 3D computational grid for Stage 2 flow modeling [cm³]

Stage-2 Lateral Flow in 3D grid

$$\Delta V_{k\leftarrow l} = \frac{\Delta t}{60}\left\{T\left[(P_l + E_l) - (P_k + E_k)\right]\left(1\,\frac{\text{ml}}{\text{cm}^3}\right) + D\left(\frac{V_l - V_k}{s^2}\right)\right\}$$

$\Delta V_{k\leftarrow l}$	Extravasated fluid volume flowing laterally into cell k from adjacent cell l during the time step [ml]
Δt	Time step [min]
s	Lateral distance between adjacent cells, side length for uniform cubic grid [cm]
P_k	Hydrostatic pressure head in cell k [cm]
P_l	Hydrostatic pressure head in cell l [cm]
E_k	Elevation head for cell k relative to the site of administration [cm]
E_l	Elevation head for cell l relative to the site of administration [cm]
V_k	Extravasated fluid volume in computational cell k [ml]
V_l	Extravasated fluid volume in computational cell l [ml]
T	Transmissivity for lateral extravasation flow within a tissue layer [$cm^2\ h^{-1}$]
D	Diffusivity of extravasated fluid in tissue [$cm^2\ h^{-1}$]

Stage-2 Vertical Flow in 3D Grid

$$\Delta V_{k\leftarrow l} = \frac{\Delta t}{60}\left[U\left(\frac{s}{d}\right)(P_l - P_k)\left(1\,\frac{\text{ml}}{\text{cm}^3}\right) + D\left(\frac{V_l - V_k}{d\ s}\right)\right]$$

$\Delta V_{k\leftarrow l}$ Extravasated fluid volume flowing vertically into cell k from adjacent cell l during the time step [ml]

U Transmissivity of vertical flow across tissue layers [$cm^2\ h^{-1}$]

d Effective vertical distance between adjacent cells for flow modeling [cm]

$$d = s + \left(\frac{V_k + V_l}{2s^2}\right)\left(1\,\frac{\text{cm}^3}{\text{ml}}\right)$$

Large volumes of infiltrating fluid increase the effective distance over which hydrostatic pressure difference acts for vertically adjacent computational cells (voxels)

V_k Extravasated fluid volume for cell k [ml]

V_l Extravasated fluid volume for cell l [ml]

s Voxel side length [cm]

Vascular-Lymphatic Removal of Extravasated Fluid

Vascular-lymphatic removal of extravasated fluid from the k^{th} computational cell (voxel) during each time step

$$V_k^- = \frac{\lambda_v \, \Delta t}{60} V_k$$

λ_v Relative vascular-lymphatic removal rate [h^{-1}]

In the current implementation, a single relative vascular-lymphatic removal rate of 0.15 h^{-1} is used in Stage 2.

If a warm compress event is included as a timeline input, a removal rate of 0.25 h^{-1} is used for that time period.

Limb Elevation Influences Relative Elevation Head Calculation

$$E_k = r_k \cos(\theta - \theta_k) \sin(\varphi)$$

- E_k Relative elevation head for the k^{th} computational cell [cm]
- r_k Radial distance of the k^{th} computational cell [cm]
- θ_k Polar angle for the computation cell arranged within the grid [degrees]
- θ Angle for the lift direction [degrees]
- φ Tissue lift angle [degrees]

User-specified angles for (left) polar angle θ for lift direction and (right) azimuthal angle φ for lift magnitude

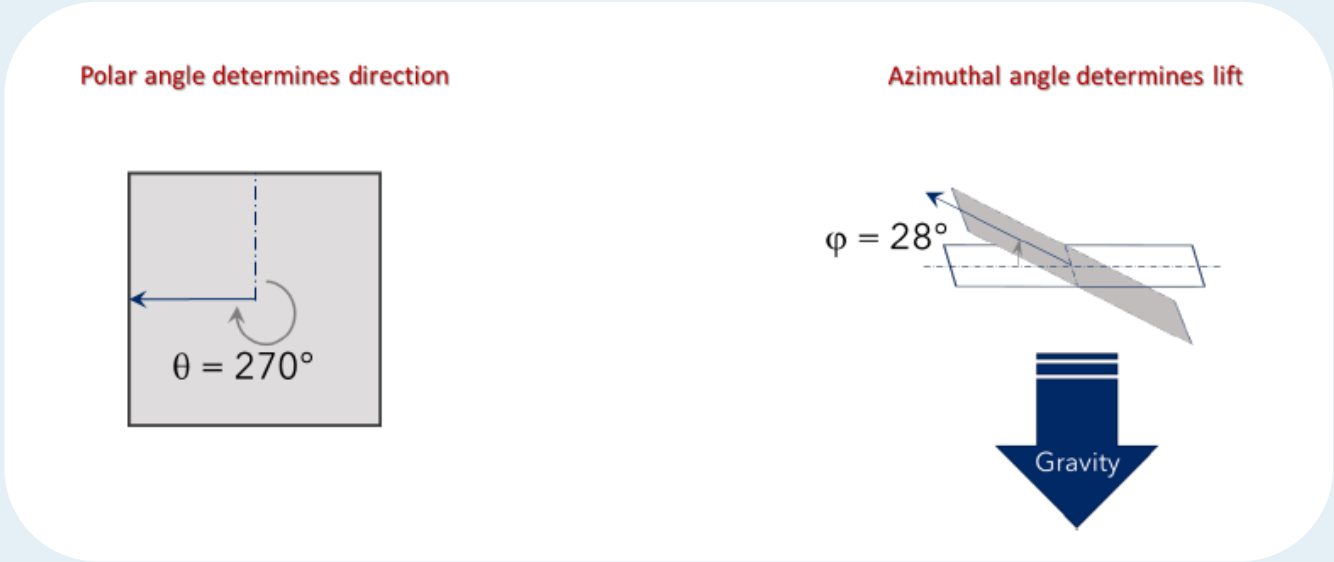

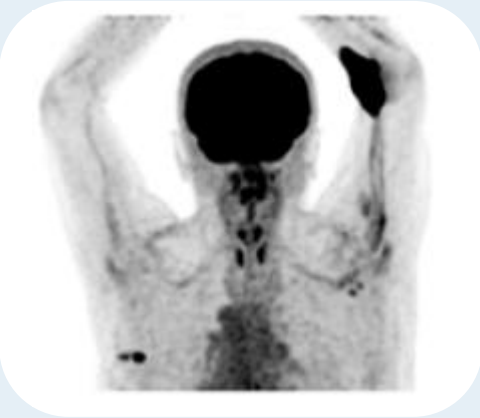

Fig. 3(C) in Iori et al. (2022) https://doi.org/10.21203/rs.3.rs-2009242/v1

Radial Distances for Elevation Head

r_k is the cell center distance to center of grid

θ_k is the polar angle for lift direction

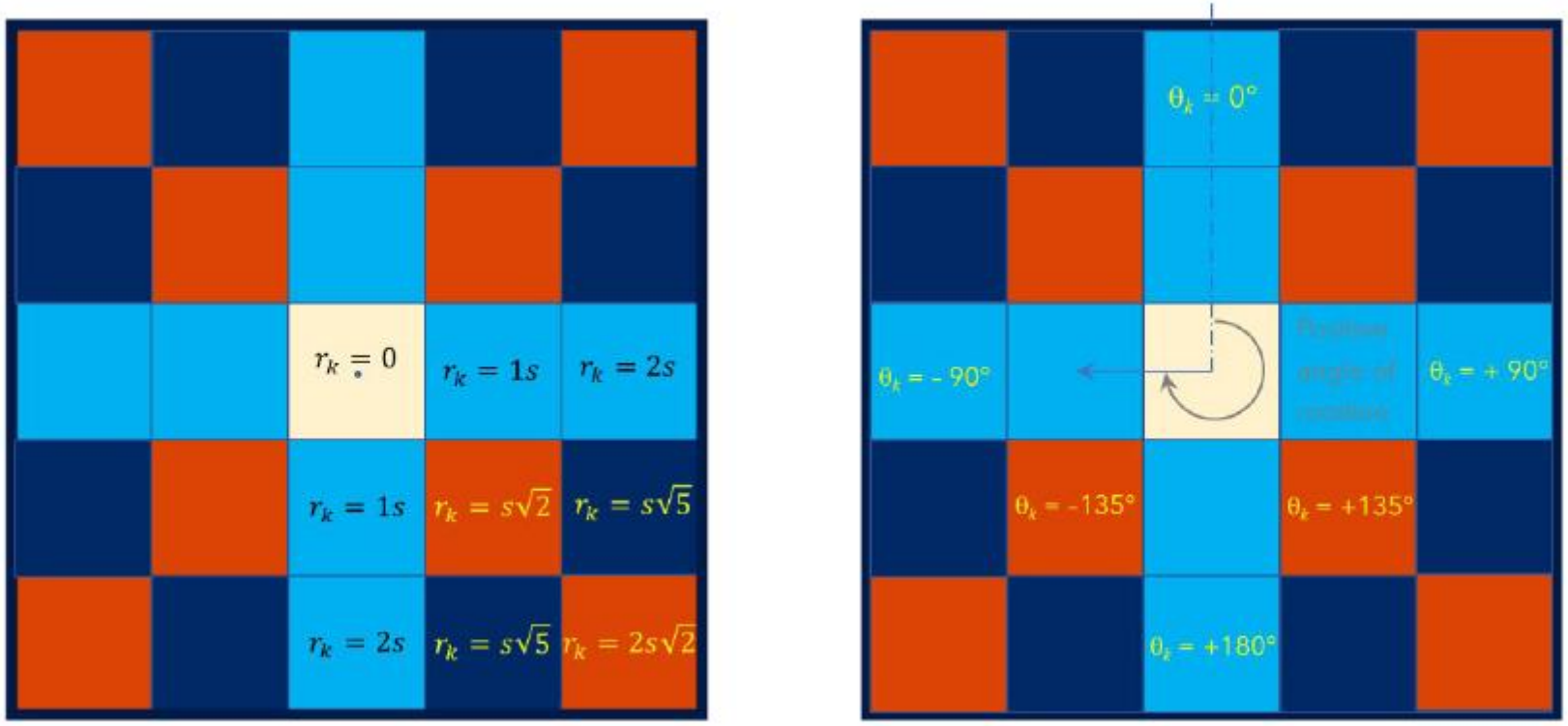

Radial distances and polar angles for a square grid with a side length s

Activity Concentration Model

Activity Concentration Model

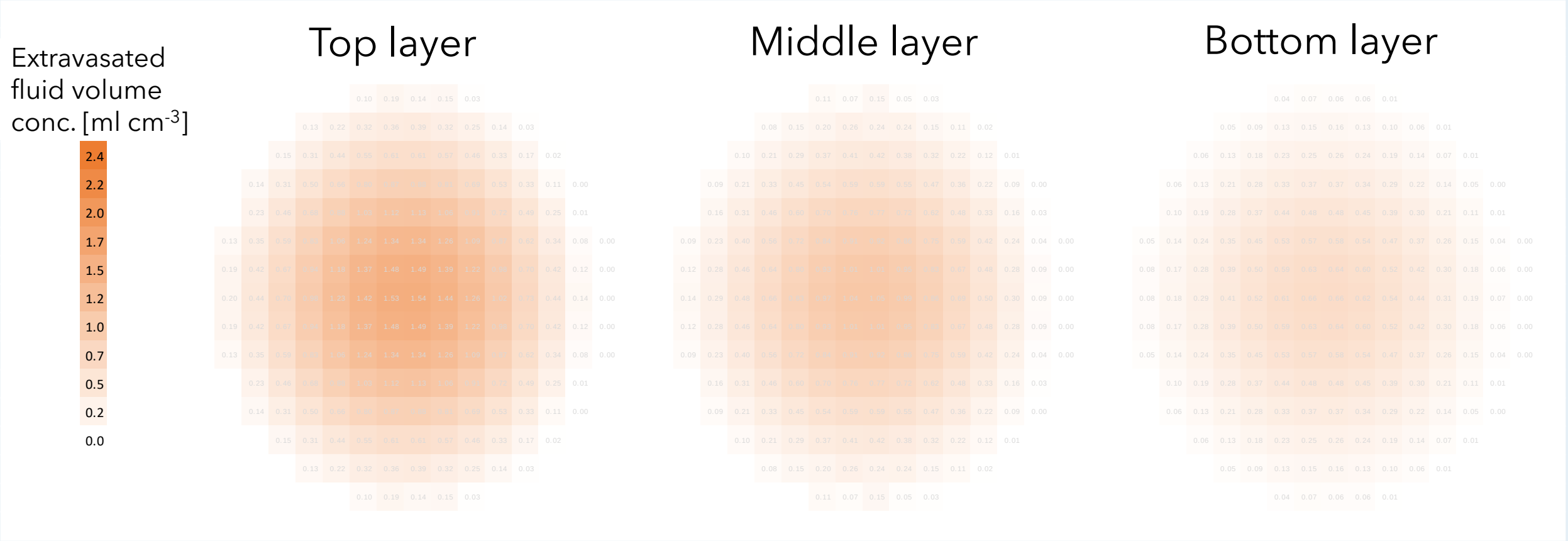

- Converts extravasated fluid in tissue (test flow result above) into activity per unit volume
- Applies 3D computational grid with unit tissue density that does not flex or deform
- Transfers spatial- & time-dependent activity concentrations in tissue to dosimetry model

V+ software is available from U.S. NRC https://ramp.nrc-gateway.gov/

Activity Concentration Parameters & Constraint

- Utilizes radiopharmaceutical activity concentration in extravasated fluid
  - Unitless fraction for nonradioactive fluid in tissue displaced during extravasation, set to 0.33 (extracellular fluid fraction)
  - No additional inputs for this model
- Biological processes do not concentrate extravasated radioactivity in tissue
- Constraint limits activity concentration in tissue

$$C^*_{k,i} \leq C$$

$C^*_{k,i}$ Activity concentration in tissue [Bq cm^{-3}]

C Activity of radiopharmaceutical per unit extravasated fluid volume [Bq ml^{-1}]

with 1 cm^3 = 1 ml

- Model considers dilution with nonradioactive fluid

Activity Concentration in Tissue

based on extravasated fluid volume in computational cells (voxels)

$$C^*_{k,i}(t) = \begin{cases} F^*_{k,i}\, Ce^{-\lambda_r \mathrm{t}} & \text{if } F^*_{k,i} \le F \\ \dfrac{1}{\left(1 + F^*_{k,i} - F\right)} F^*_{k,i}\, Ce^{-\lambda_r \mathrm{t}} & \text{if } F^*_{k,i} > F \end{cases}$$

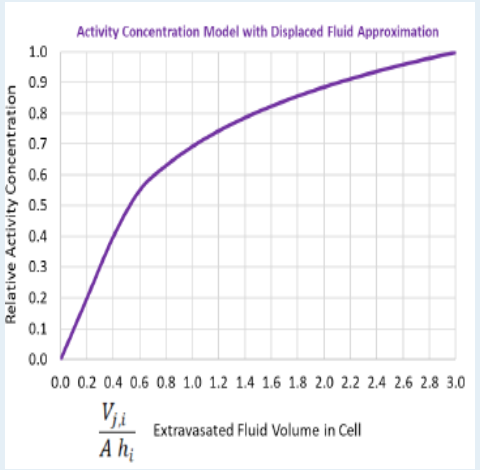

$C^*_{k,i}(t)$ Activity concentration in tissue [Bq cm^{-3}] at time t [min]

C Activity of radiopharmaceutical per unit extravasated fluid volume [Bq ml^{-1}]

$F^*_{k,i}$ Extravasated fluid at the location expressed as a fraction of the computational cell volume [unitless], $F^*_{k,i} = \left(\frac{V_{k,i}}{s^3}\right)\left[\frac{ml}{cm^3}\right]$ where 1 cm^3 = 1 ml

$V_{k,i}$ Extravasated fluid volume in a computational cell at the k^{th} location in the i^{th} layer, output from the extravasation flow model [ml]

s Lateral distance between adjacent cells, side length for uniform cubic grid [cm]

F Fraction of nonradioactive fluid in tissue that is displaced during extravasation, $0 \le F \le 1$ [unitless]

λ_r Radioactive decay constant, relative rate of removal [min^{-1}]

Part III: Dosimetry Model

Extravasation Dosimetry in the Literature

- Generally, methods involve self-absorption assumptions in spheres of various size (i.e., “affected volume”)
- Modeling may include time-dependent removal of extravasated radioactivity from the affected volume
- The pharmaceutical (chemical structure) is very important for determining biological loss rates
- Deterministic threshold doses on the order of 2-20 Gy for erythema, epilation, edema, desquamation, blistering, ulceration, burns, and necrosis.

Activity Model for Dose Estimation

– Dosimetry assumptions

- biological outcome is deterministic
- homogeneous tissue (ρ = 1.1 g/cm^3) containing both source and target
- 3D grid structure of fine cubic cells with specified side length, s
- gross volume of “affected tissue” W x L x D
- concentration per cell as a function of time passed from transport model

– Activity in a given voxel is proportional to radiopharmaceutical concentration

$$A_{k,i}(t) = C^*_{k,i}(t) \cdot s^3$$

kth location in the ith layer

Number of Dosimetry Calculations

- Considering contributions from photons, electrons, and alpha
- Generally, using point-kernel methods with two considerations:
  - energy self-absorption in each voxel
  - emissions from a source voxel to energy absorption in a distant target voxel
- A very large number of dose calculations are carried out:
  - for example, an affected volume of 20 x 40 x 1 calculational cells results in about 5.8M dosimetry calculations for each time step
  - In Phase 1
    - one time step for each simulated second
  - In Phase 2
    - the number of time steps is dependent on fluid velocity (Courant-number limited)
    - there could be tens-to-hundreds of time-steps per simulated minute

Extravasation Photon Dosimetry

- The point-kernel method is implemented for photons
- For self-absorption and distant energy deposition
- Photon absorbed dose rate (Gy s^{-1}) at distance *r*, is calculated as shown below

$$\dot{D}_\gamma(r) = \frac{k\ A\ Y\ E_0}{4\pi\ r^2}\left(\frac{\mu_{en}}{\rho}\right)e^{-\mu r}$$

k	unit conversion [1.6×10^{-10} J g MeV^{-1} kg^{-1}]
A	activity in the calculational cell [nt s^{-1}]
Y	emission yield [γ nt^{-1}]
E_0	uncollided photon energy [MeV γ^{-1}]
r	point-kernel distance [cm]
$\frac{\mu_{en}}{\rho}$	mass energy absorption coefficient [cm^2 g^{-1}]
μ	linear attenuation coefficient [cm^{-1}]

Self-Absorption in the Source Voxel

Given a unit cube, we can randomly sample multiple combinations of source and target points. The distance between the two points is related to r (i.e., the probability of r, *p(r)*) in the point-kernel equation. The distribution of these random point kernel distances is referred to as a point-pair distribution.

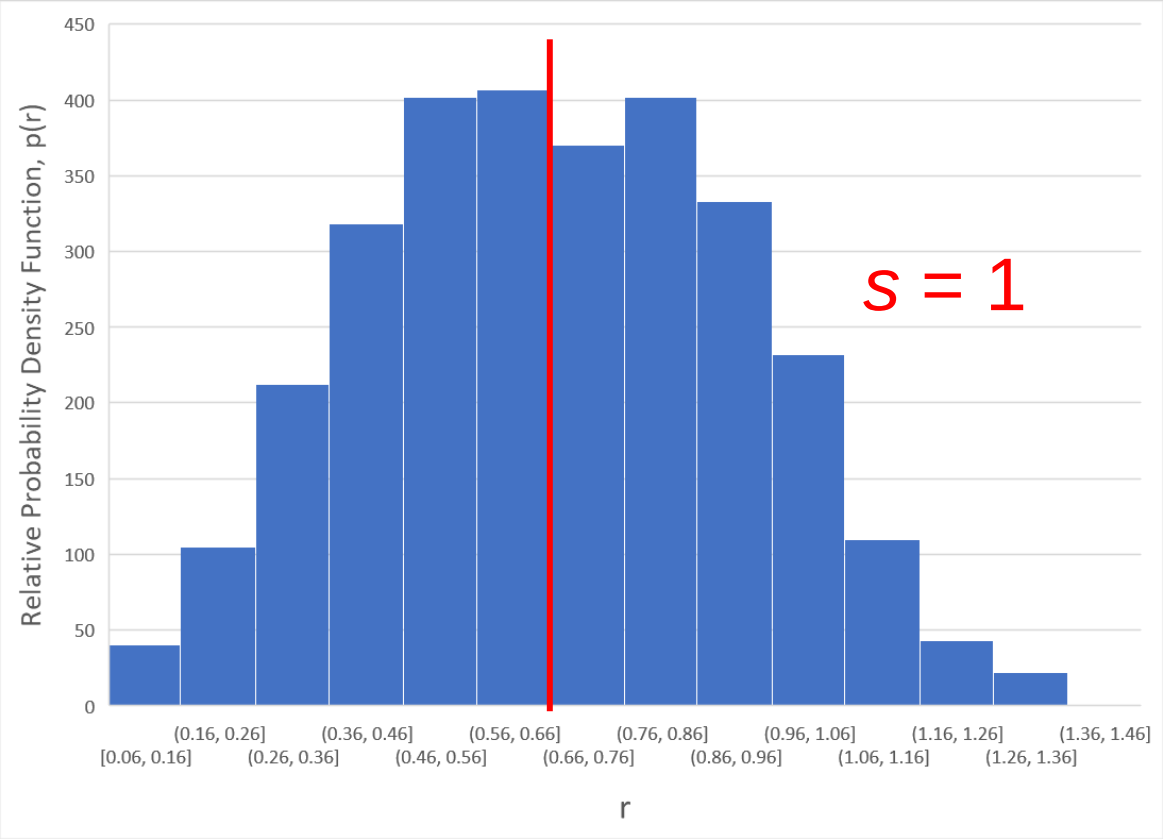

Based on the histogram, the point-kernel distance used for cells that are both source and target is assumed to be two-thirds of voxel side length specified by the user (i.e., $r = \frac{2}{3}s$).

Distant Voxels

Source (S) emissions represented at voxel center

Target (T) receptor represented at voxel center

Dose calculated by point kernel method using distance, r

When source and target are different cells, distance between computational cells, r, with centroid 3D coordinates of (x_1, y_1, z_1) and (x_2, y_2, z_2), is calculated as

$$r = \sqrt{(x_2 - x_1)^2 + (y_2 - y_1)^2 + (z_2 - z_1)^2}$$

With non-adjacent voxels, this point-kernel method works well, i.e., to within 10% of Monte Carlo volume-to-volume methods.

Extravasation Electron Dosimetry

– Electron dosimetry methods utilize the SkinDose (V+) SADCALC routine with this point kernel:

$$\dot{D}_e(r) = k\frac{A\,Y\,\bar{E}_e\,F_e(\delta, E_o)}{\rho\,4\pi\,r^2\,X_{90}}$$

– With these additional parameters:

- X_{90} = distance from source in which 90% of electron energy is deposited [cm]
- $F_e(\delta, E_o)$ = scaled absorbed dose distribution (SADD) [unitless]
- δ is the scaling index for point-kernel distance (i.e., $^{r}/_{X_{90}}$)

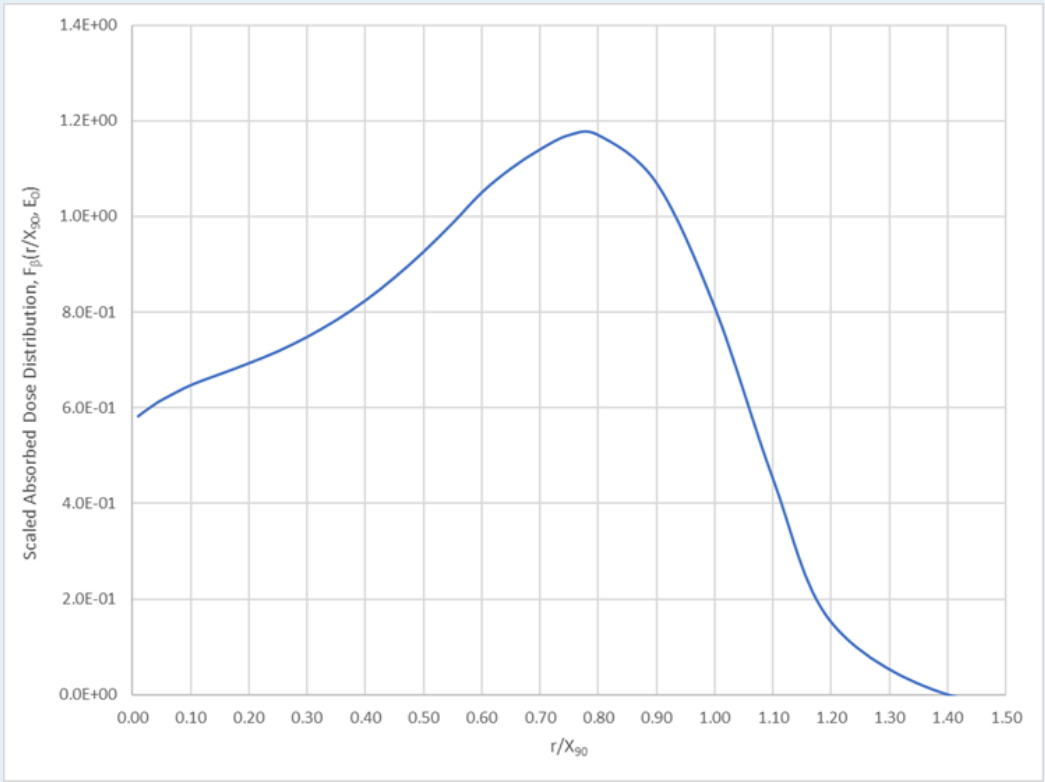

Similar to photons

- For instances where source and target are the same voxel, again the assumption applies: $r = \frac{2}{3}s$
- In cases where the X_{90} is very short relative to the cubic side ($X_{90} < \frac{s}{4.5}$), the electron energy is shown to be completely absorbed in the source voxel, thus:

$$\dot{D}_e = k\frac{A\,Y\,\bar{E}_e}{\rho\,s^3}$$

Extravasation Alpha Dosimetry

- Alpha particles travel no more than about 100 microns in tissue
  - recoil atoms also carry kinetic energy, but in even shorter distances
- Therefore, the point-kernel method is not appropriate
- An energy-balance method is used instead
- The majority of emitted alpha energy is absorbed in the source voxel (self absorption)
  - with a small fraction assumed to be absorbed in one of the six adjacent voxels
- Alpha dosimetry is dependent on alpha range
  - i.e., what fraction of energy from the source voxel enters an adjacent voxel

Alpha energy leaving the source voxel

- Alpha emissions from a given source are uniformly distributed in a source voxel. Given the alpha range, R, and the voxel side dimension, s, the volume of the shell in the source voxel from which these alphas can escape to adjacent voxels is determined.
- For alpha emissions originating in that shell, we would expect roughly ½ to be direct into the voxel and the other ½ directed out of the voxel.
- The energy fraction transported to one of six adjacent voxels is calculated.
- This fraction is dependent on the source voxel dimension, s, and the alpha range, R

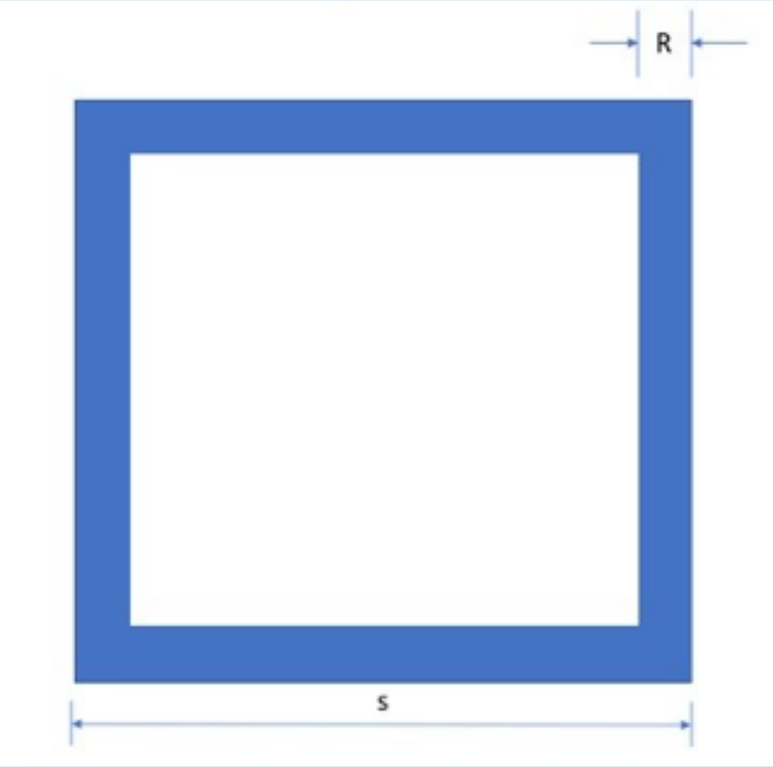

Alpha Dosimetry

– Alpha absorbed dose rate to the source voxel is:

$$\dot{D}_{\alpha S} = k\frac{A\,Y\,E_{\alpha}}{\rho\,s^3}\left(1 - {}^{3R}/_{s}\right)$$

– Alpha dose rate to <u>each</u> of the adjacent voxels is:

$$\dot{D}_{\alpha A} = k\frac{A\,Y\,E_{\alpha}}{\rho\,s^3}\left({}^{R}/_{2s}\right)$$

For R = 0.005 cm and s = 1 cm,

$$\left(1 - \frac{3R}{s}\right) = 0.985$$

and

$$\left(\frac{R}{2s}\right) = 0.0025$$

Main Component Highlights

Benjegerdes et al. (2017) Focal cutaneous squamous cell carcinoma following Radium-223 extravasation. Baylor University Medical Center Proceedings 30:1, 78-79, DOI: 10.1080/08998280.2017.11929538.

Local Tissue Dose from Extravasation

- Flow Model
  - Stage 1 during Radiopharmaceutical Administration
  - Stage 2 after Radiopharmaceutical Administration
- Activity Concentration Model
- Dosimetry Model

Presently not included in ExtravDose calculations

- Basal layer dose
- Decay progeny dose contributions

Questions